

See discussions, stats, and author profiles for this publication at: <https://www.researchgate.net/publication/235887098>

# Charge-Transfer Complexes between $\text{NH}_3$ and the Halogens $\text{F}_2$ , $\text{ClF}$ , and $\text{Cl}_2$ : An ab Initio Study on the Intermolecular Interaction

ARTICLE in THE JOURNAL OF PHYSICAL CHEMISTRY A · JULY 2000

Impact Factor: 2.69 · DOI: 10.1021/jp000922o

---

CITATIONS

64

---

READS

32

## 1 AUTHOR:



Alfred Karpfen

University of Vienna

162 PUBLICATIONS 4,273 CITATIONS

SEE PROFILE

# Charge-Transfer Complexes between NH<sub>3</sub> and the Halogens F<sub>2</sub>, ClF, and Cl<sub>2</sub>: An ab Initio Study on the Intermolecular Interaction

Alfred Karpfen\*

Institut für Theoretische Chemie und Molekulare Strukturbioogie der Universität Wien, A-1090 Wien, Währingerstrasse 17, Austria

Received: March 9, 2000; In Final Form: May 3, 2000

The ground-state properties of the charge transfer complexes formed between NH<sub>3</sub> and the halogens F<sub>2</sub>, ClF, and Cl<sub>2</sub> were investigated systematically with the aid of ab initio calculations. Extended basis sets were applied and electron correlation was included at different levels of Møller–Plesset perturbation theory and coupled cluster expansions. Not only the level of electron correlation and the basis set chosen are important, but also the use of the counterpoise correction to the basis set superposition error directly in the course of the geometry optimization has a significant influence on the calculated equilibrium structures. The trends in other ground-state properties of these complexes, such as vibrational spectra, infrared intensities, selected harmonic force constants, dipole moments, and nuclear quadrupole coupling constants are discussed and compared to experimental data. The strength of the intermolecular interaction in this series increases in the order NH<sub>3</sub>–F<sub>2</sub>, NH<sub>3</sub>–Cl<sub>2</sub>, and NH<sub>3</sub>–ClF.

## Introduction

The structures of the gas-phase complexes between NH<sub>3</sub> and the halogen molecules F<sub>2</sub>, ClF, and Cl<sub>2</sub> have been investigated quite recently with the aid of rotational spectroscopic experiments.<sup>1–3</sup> The properties of the heterodimers formed between amines and halogens have usually been discussed in the context of electron donor–acceptor (EDA) or charge-transfer (CT) complexes. For the above three complexes the signature of CT increases in the series NH<sub>3</sub>–F<sub>2</sub>, NH<sub>3</sub>–Cl<sub>2</sub>, NH<sub>3</sub>–ClF. However, the case of NH<sub>3</sub>–F<sub>2</sub> can be well understood as that of a weakly bound complex with almost vanishing charge-transfer contributions, and even NH<sub>3</sub>–ClF has been described as a complex with only a small contribution from the ionic valence bond structure [H<sub>3</sub>NCI]<sup>+</sup>...F<sup>–</sup>.<sup>2</sup> So far, because of the extreme reactivity of ammonia with halogens, experimental gas-phase vibrational spectra of these *prereactive* complexes are not available yet. Matrix isolation studies have, however, been reported for the case of NH<sub>3</sub>–F<sub>2</sub><sup>4</sup> and NH<sub>3</sub>–ClF.<sup>5</sup>

Several theoretical investigations have already been performed on these complexes: NH<sub>3</sub>–F<sub>2</sub>,<sup>6–16</sup> NH<sub>3</sub>–ClF,<sup>6,7,9,11–14,17,18</sup> and NH<sub>3</sub>–Cl<sub>2</sub>.<sup>6,7,9,11–14,17–19</sup> With the exception of the early self-consistent field (SCF) calculations,<sup>6,7,17</sup> most of the later treatments have been done at the Møller–Plesset second-order (MP2)<sup>20</sup> level or using density functional theory (DFT) variants. A notable exception is the work of Røeggen and Dahl<sup>9</sup> in which an extended geminal model was applied.

In the most recent investigation on NH<sub>3</sub>–F<sub>2</sub>,<sup>16</sup> an unexpectedly large sensitivity of the calculated complex properties to the level of electron correlation emerged. The range of calculated intermolecular distances  $R(\text{N}\cdots\text{F})$  varied by about 0.3 Å when comparing the results of different Møller–Plesset and coupled cluster variants. Moreover, as far as the calculated equilibrium intermolecular distance is concerned, the explicit use of the counterpoise (CP) correction<sup>21</sup> to the basis set superposition error

(BSSE) in the course of the geometry optimization turned out to be important, too.

This work aims toward a consistent description of the equilibrium structures and the vibrational spectra of these three complexes at a reliable methodical level, thereby exploring the effect of higher-order electron correlation contributions. Instead of attempting a detailed analysis and assessment of the amount of charge transfer in these complexes either via population analysis, integrations of the electron density, or energy partitioning schemes, other ground-state properties such as dipole moments, selected harmonic force constants, and electric field gradients are computed and used to characterize the intermolecular interaction in these complexes. Further goals of this study are to clarify whether this striking sensitivity with respect to the correlation method chosen persists for the other two complexes as well, and whether the application of the CP correction in the course of the geometry optimization leads to significant structural effects. These aspects are important for future studies on the interaction of halogens with substituted amines, and probably also for other CT complexes, where the explicit consideration of extended basis sets in combination with electron correlation contributions beyond MP2 will, in general, be too costly and strongly limited by the available computing resources.

## Method of Calculation

In this work, all quantum chemical calculations were performed with the Gaussian 98<sup>22</sup> suite of programs. The MP2 method and a series of approaches taking account higher-order electron correlation contributions up to MP4(SDTQ)<sup>23</sup> and CCSD(T)<sup>24–28</sup> were applied. Several extended basis sets were tried. Here, only the results as obtained with the 6-31++G-(d,p), 6-311++G(2d,2p), 6-311++G(3df,2p),<sup>29–34</sup> and aug-cc-pVTZ<sup>35–37</sup> basis sets are reported. Structural results for the NH<sub>3</sub>–F<sub>2</sub> complex as obtained with the first three of these basis sets have already been reported.<sup>16</sup> Geometry optimizations were carried out using analytical gradients where available. In the

\* Corresponding author. Tel: (+43-1) 4277-52760. Fax: (+43-1) 4277-9527. E-mail: Alfred.Karpfen@univie.ac.at.

case of MP4(SDTQ), CCSD, QCISD(T), and CCSD(T) calculations the gradients were determined numerically. Only in the case of the  $\text{NH}_3\text{--Cl}_2$  complex did post-MP2 calculations with the aug-cc-pVTZ basis set surpass the available computing resources. Harmonic vibrational frequencies were determined at the MP2 level only. The CP correction to the BSSE was not calculated as a correction at the respective optimized geometries but was computed at each point of pointwise evaluated energy surfaces. Because of the negligibly small geometry relaxation of the  $\text{NH}_3$  moiety in these three complexes relative to the free  $\text{NH}_3$  molecule, the scans of the energy surfaces could be reduced to those of 2D problems with the intermolecular  $R(\text{N}\cdots\text{X})$  distance and the intramolecular halogen distance  $R(\text{X--Y})$  as parameters without significant loss of accuracy. The  $\text{NH}_3$  structure used in these 2D scans was mostly the one obtained from global CCSD(T) optimizations of the complex within a given basis set. Only in the case of the larger two basis sets were the corresponding MP2 structures of the  $\text{NH}_3$  moiety used. The difference appears to be negligible. The importance of including the CP correction in the course of the geometry optimization has been discussed quite recently in the case of hydrogen-bonded complexes<sup>38,39</sup> and has also been encountered in the recent study on  $\text{NH}_3\text{--F}_2$ .<sup>16</sup>

## Results and Discussion

**A. The Monomers.** One of the key requirements for reliable calculations of the structure and of other properties of the charge-transfer complexes between amines and halogens is a reasonably correct description of the equilibrium structure of the halogens. Whereas the description of the  $\text{NH}_3$  molecule is quite unproblematic, with structure variations well below 0.01 Å in the N–H distances and below 1° in the HNH bond angle when applying the above four basis sets and the different electron correlation techniques, the sensitivity of the equilibrium distance of the halogen to the methodical level applied is considerably higher. To illustrate this point, the dependence of the computed  $R(\text{F--F})$ ,  $R(\text{Cl--F})$ , and  $R(\text{Cl--Cl})$  values of  $\text{F}_2$ ,  $\text{ClF}$ , and  $\text{Cl}_2$  on the electron correlation method applied are shown in Figure 1. MP2- and CCSD(T)-calculated equilibrium distances are confronted with experimental values in Table 1. As a general trend, the computed equilibrium distances are somewhat too large, even with the two largest basis sets. Since the use of even more extended basis sets is prohibitive for the complexes, these methodical errors have to be accepted at the current stage. Because of the very weak structure modification of the  $\text{NH}_3$  moiety and because of the close agreement to the experimental structure, the computed  $\text{NH}_3$  structural data are not reported in detail in the following.

**B. The CT Complexes.** At all computational levels probed in this work each of the three  $\text{NH}_3\text{--XY}$  complexes has an optimized geometry with  $C_{3v}$  symmetry and, hence, with a linear  $\text{N}\cdots\text{X--Y}$  structure (see Figure 2). Before going to a detailed discussion of the results for each of the complexes, the comparatively high sensitivity of the computed intermolecular  $\text{N}\cdots\text{X}$  distance to the level of electron correlation applied is illustrated. In Figure 3, the computed  $\text{N}\cdots\text{X}$  distances of the three CT complexes are compared to the optimized  $\text{N}\cdots\text{X}$  distances of the hydrogen-bonded dimers  $\text{NH}_3\text{--HF}$  and  $\text{NH}_3\text{--HCl}$ . Results for nine different electron correlation variants are shown. All these results were obtained with the 6-311++G-(2d,2p) basis set and without performing the CP correction. The resulting  $\text{N}\cdots\text{X}$  distances vary only by about 0.02 Å in the case of  $\text{NH}_3\text{--HF}$ <sup>16</sup> and 0.09 Å in the case of  $\text{NH}_3\text{--HCl}$ . In sharp contrast to these hydrogen-bonded dimers, a much larger

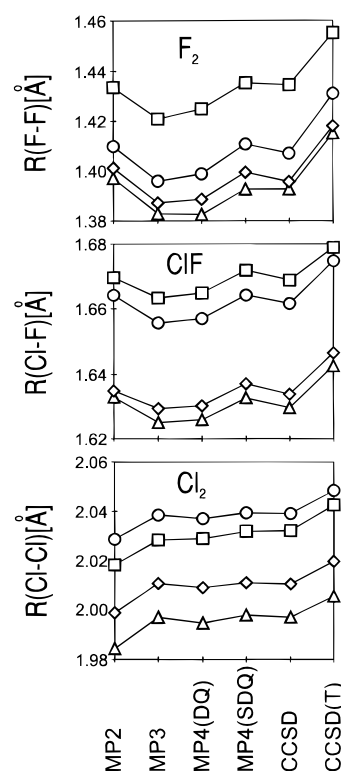


**Figure 1.** Computed equilibrium distances of  $\text{F}_2$ ,  $\text{ClF}$ , and  $\text{Cl}_2$  as obtained with different electron correlation methods and different basis sets: (squares) 6-31++G(d); (circles) 6-311++G(2d); (triangles) 6-311++G(3df); (diamonds) aug-cc-pVTZ.

**TABLE 1: Calculated MP2 and CCSD(T) and Experimental Equilibrium Distances of  $\text{F}_2$ ,  $\text{ClF}$ , and  $\text{Cl}_2$  (Å)**

basis set	method	$\text{F}_2$	$\text{ClF}$	$\text{Cl}_2$
6-31++G(d)	MP2	1.4336	1.6697	2.0180
	CCSD(T)	1.4551	1.6790	2.0425
6-311++G(2d)	MP2	1.4099	1.6642	2.0286
	CCSD(T)	1.4311	1.6747	2.0484
6-311++G(3df)	MP2	1.3972	1.6330	1.9845
	CCSD(T)	1.4152	1.6426	2.0054
aug-cc-pVTZ	MP2	1.4013	1.6348	1.9987
	CCSD(T)	1.4181	1.6464	2.0195
exp <sup>a</sup>		1.4176	1.6318	1.9920
exp <sup>b</sup>		1.4119	1.6283	1.9879

<sup>a</sup> Calculated from experimental  $B_0$  values as reported in refs 1-3.

<sup>b</sup> Reference 40.

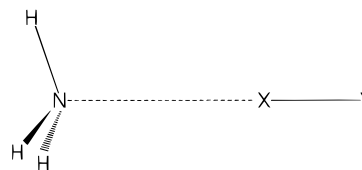


**Figure 2.** Sketch of the  $C_{3v}$  equilibrium structure of the  $\text{NH}_3\text{--XY}$  complexes.

variation is encountered in the CT complexes, with about 0.3 Å for  $\text{NH}_3\text{--F}_2$ <sup>16</sup> and slightly less than 0.2 Å for  $\text{NH}_3\text{--ClF}$  and  $\text{NH}_3\text{--Cl}_2$ . Already from this first comparison it becomes clear that the MP2 results for all three CT complexes are, in general, in better agreement with those electron correlation methods, which take account of triple excitations, MP4(SDTQ) and CCSD(T).

To further illustrate the effect of triple excitations for the three CT complexes and the two hydrogen-bonded dimers, the results as obtained with MP2, MP4(SDQ), MP4(SDTQ), QCISD, QCISD(T), CCSD, and CCSD(T) applying the 6-311++G-

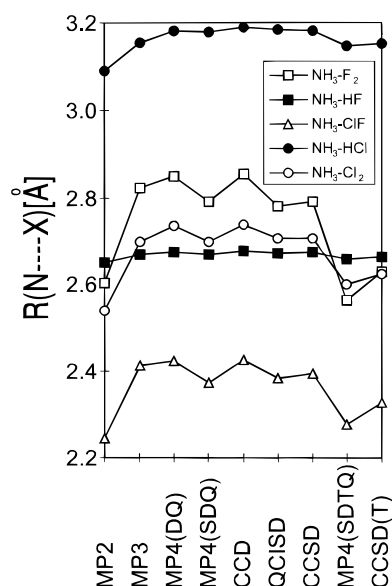


**Figure 3.** Inter-molecular  $R(N\cdots X)$  distance of hydrogen-bonded and CT complexes as obtained with the 6-311++G(2d,2p) basis and different electron correlation methods.

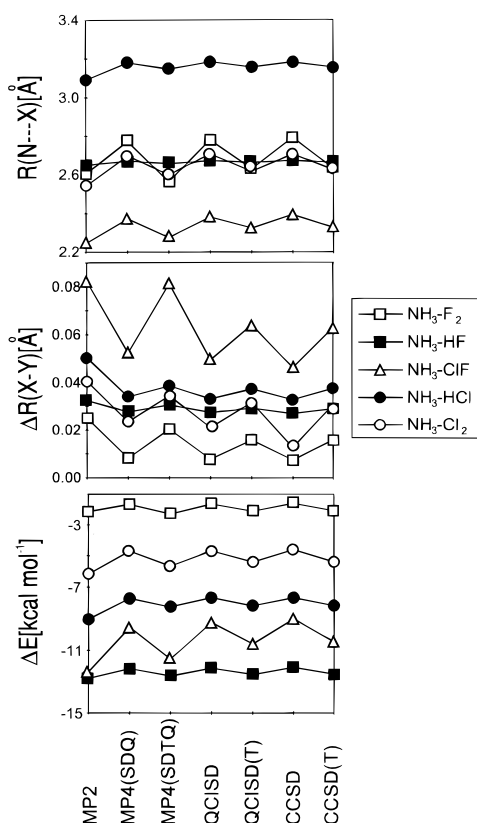


**Figure 4.** Inter-molecular  $R(N\cdots X)$  distance, widening of the intramolecular  $R(X-Y)$  distance, and interaction energy  $\Delta E$  of hydrogen-bonded and CT complexes as obtained with the 6-311++G(2d,2p) basis and different electron correlation methods.

(2d,2p) basis and again without CP correction are reported. In Figure 4, the trends for the intermolecular distances  $R(N\cdots X)$ , for the widening of the intramolecular distances  $\Delta R(X-Y)$  ( $\Delta R(H-X)$  in the case of the hydrogen-bonded dimers) and for the intermolecular interaction energy, are shown graphically. Figure 4 clearly demonstrates that (i) there is a distinct difference between the methods that take account of triple excitations, and the post-MP2 methods which do not and (ii) the results taking

account of triples are bracketed by the MP2 numbers and the results obtained without triples.

**NH<sub>3</sub>-F<sub>2</sub>.** In Table 2, the computed  $R(N\cdots F)$  values of the NH<sub>3</sub>-F<sub>2</sub> complex are compiled. Results as obtained from calculations without and with the inclusion of the CP correction in the course of the geometry optimization are shown. The corresponding optimized intramolecular  $R(F-F)$  values are collected in Table 3. MP2/6-31++G(d,p) calculations without CP correction produce a complex geometry with almost equal  $R(N\cdots F)$  and  $R(F-F)$  distances, halfway to the gas-phase ion pair.<sup>16</sup> This is an artifact. At all other levels of approximation an intermolecular complex with only a weak perturbation of the intramolecular F-F distance is obtained. The differences in the structural predictions when applying different post-MP2 approaches are quite substantial. These trends do not change when improving the basis set. The modification of the equilibrium structure when including the CP correction is significant; however, it remains nearly constant for a given basis set. This correction is nonnegligible, even with the aug-cc-pVTZ basis set but it is reduced to 0.04 Å. The best computed value of 2.67 Å for the intermolecular  $R(N\cdots F)$  distance as obtained at the CP-corrected CCSD(T)/aug-cc-pVTZ level is somewhat shorter than the experimentally deduced 2.708 Å.<sup>1</sup> With the exception of MP2 all other approaches lead to the prediction of much larger intermolecular distances. The computed lengthening of the intramolecular  $R(F-F)$  distance amounts to 0.012 Å at the CCSD(T)/aug-cc-pVTZ level. Again, the MP2 value is close to the CCSDT results, all other approaches lead to significantly smaller elongations. The inclusion of triple excitations appears to be decisive to achieve agreement with experiment; the close agreement between the optimized MP2 and CCSD(T) structure for NH<sub>3</sub>-F<sub>2</sub> is a bit fortuitous. Upon complex formation the HNH bond angles are widened by about 0.1° only.

The computed stabilization energies are collected in Table 4. The trends parallel exactly those discussed for the complex geometry. For a given basis set MP2 and CCSD(T) stabilization energies are very close; those for the other correlation methods lead to less intermolecular binding by about 0.5 kcal mol<sup>-1</sup> considering CP-corrected energies. The use of the aug-cc-pVTZ basis drastically reduces the CP correction. At the CCSD(T)/aug-cc-pVTZ level the predicted stabilization energy amounts to -1.70 kcal mol<sup>-1</sup> with a still nonnegligible CP correction of 0.3 kcal mol<sup>-1</sup>.

Computed harmonic vibrational spectra and infrared intensities of the NH<sub>3</sub>-F<sub>2</sub> complex as obtained with the three larger basis sets at the MP2 level together with the frequency shifts relative to the monomers are shown in Table 5. The four highest-lying frequencies originate completely from the ammonia subunit. More important than the absolute values of the frequencies are the shifts relative to the computed frequencies of the NH<sub>3</sub> molecule, as obtained at the same methodical level. With all three basis sets, the qualitative description of these shifts is very similar. The N-H stretching modes and the degenerate deformation mode are hardly modified or slightly red-shifted, whereas the totally symmetric deformation mode is blue-shifted by about 8 cm<sup>-1</sup>. These small shifts are fully in line with the very weak structure change of the NH<sub>3</sub> subunit upon complex formation. The intramolecular F-F stretching mode on the other hand is strongly red-shifted by about -100 cm<sup>-1</sup> relative to the F<sub>2</sub> monomer mode. The MP2 results for the F<sub>2</sub> harmonic stretching frequency as obtained with the three larger basis sets are with 964, 989, and 1038 cm<sup>-1</sup>, respectively, all considerably higher than the *experimental harmonic* frequency of 916 cm<sup>-1</sup> or the gas-phase fundamental of 895

**TABLE 2: Calculated Intermolecular Distances of the CT Complex NH<sub>3</sub>–F<sub>2</sub> As Obtained with Different Electron Correlation Methods, with Different Basis Sets, and without,  $R(N\cdots F)$ , and with,  $R_{CP}(N\cdots F)$ , CP Correction (Å)**

basis set		MP2	MP3	MP4(DQ)	MP4(SDQ)	CCSD	CCSD(T)
6-31++G(d,p) <sup>a</sup>	$R(N\cdots F)$	1.85	2.69	2.71	2.64	2.65	2.48
	$R_{CP}(N\cdots F)$	2.62	2.84	2.87	2.78	2.80	2.65
	$\Delta R(CP)$	0.77	0.15	0.14	0.14	0.15	0.17
	$\Delta R(CP)$	0.11	0.09	0.09	0.09	0.09	0.11
6-311++G(2d,2p) <sup>a</sup>	$R(N\cdots F)$	2.60	2.82	2.85	2.77	2.79	2.63
	$R_{CP}(N\cdots F)$	2.71	2.91	2.94	2.86	2.88	2.74
	$\Delta R(CP)$	0.11	0.09	0.09	0.09	0.09	0.11
	$\Delta R(CP)$	0.13	0.09	0.10	0.09	0.10	0.11
6-311++G(3df,2p) <sup>a</sup>	$R(N\cdots F)$	2.57	2.78	2.81	2.74	2.75	2.60
	$R_{CP}(N\cdots F)$	2.70	2.87	2.91	2.83	2.85	2.71
	$\Delta R(CP)$	0.13	0.09	0.10	0.09	0.10	0.11
	$\Delta R(CP)$	0.13	0.09	0.10	0.09	0.10	0.11
aug-cc-pVTZ <sup>b</sup>	$R(N\cdots F)$	2.61	2.80	2.84	2.75	2.78	2.63
	$R_{CP}(N\cdots F)$	2.65	2.84	2.87	2.80	2.84	2.67
	$\Delta R(CP)$	0.04	0.04	0.03	0.05	0.06	0.04
	$\Delta R(CP)$	0.04	0.04	0.03	0.05	0.06	0.04

<sup>a</sup> Taken from ref 16. <sup>b</sup> This work.**TABLE 3: Calculated Intramolecular Distances of the CT Complex NH<sub>3</sub>–F<sub>2</sub> As Obtained with Different Electron Correlation Methods, with Different Basis Sets, and without,  $R(FF)$ , and with,  $R_{CP}(FF)$ , CP Correction (Å)**

basis set		MP2	MP3	MP4(DQ)	MP4(SDQ)	CCSD	CCSD(T)
6-31++G(d,p) <sup>a</sup>	$R(FF)$	1.686	1.430	1.433	1.448	1.445	1.480
	$R_{CP}(FF)$	1.449	1.427	1.428	1.443	1.441	1.472
	$\Delta R(CP)$	0.237	0.003	0.005	0.005	0.004	0.008
	$\Delta R_{mon}$ <sup>b</sup>	0.015	0.006	0.003	0.008	0.007	0.015
6-311++G(2d,2p) <sup>a</sup>	$R(FF)$	1.426	1.402	1.404	1.419	1.414	1.447
	$R_{CP}(FF)$	1.421	1.401	1.402	1.418	1.411	1.443
	$\Delta R(CP)$	0.005	0.001	0.002	0.001	0.003	0.004
	$\Delta R_{mon}$	0.011	0.005	0.003	0.007	0.004	0.012
6-311++G(3df,2p) <sup>a</sup>	$R(FF)$	1.414	1.390	1.389	1.403	1.400	1.430
	$R_{CP}(FF)$	1.409	1.388	1.388	1.402	1.398	1.428
	$\Delta R(CP)$	0.005	0.002	0.001	0.001	0.002	0.002
	$\Delta R_{mon}$	0.012	0.005	0.005	0.009	0.005	0.013
aug-cc-pVTZ <sup>c</sup>	$R(FF)$	1.418	1.395	1.393	1.409	1.402	1.432
	$R_{CP}(FF)$	1.415	1.393	1.391	1.407	1.400	1.430
	$\Delta R(CP)$	0.003	0.002	0.002	0.002	0.002	0.002
	$\Delta R_{mon}$	0.014	0.006	0.002	0.008	0.004	0.012

<sup>a</sup> Taken from ref 16. <sup>b</sup> Lengthening of  $R(F-F)$  in the complex (with CP correction) relative to the F<sub>2</sub> monomer. <sup>c</sup> This work.**TABLE 4: Calculated Stabilization Energies of the CT Complex NH<sub>3</sub>–F<sub>2</sub> As Obtained with Different Electron Correlation Methods, with Different Basis Sets, and without,  $\Delta E$ , and with,  $\Delta E(CP)$ , CP Correction (kcal mol<sup>-1</sup>)**

basis set		MP2	MP3	MP4(DQ)	MP4(SDQ)	CCSD	CCSD(T)
6-31++G(d,p) <sup>a</sup>	$\Delta E$	-4.50	-2.55	-2.46	-2.79	-2.70	-3.42
	$\Delta E(CP)$	-1.75	-1.20	-1.15	-1.37	-1.31	-1.71
	$\Delta\Delta E$	2.75	1.35	1.31	1.42	1.39	1.71
	$\Delta\Delta E$	0.67	0.55	0.52	0.56	0.56	0.69
6-311++G(2d,2p) <sup>a</sup>	$\Delta E$	-2.12	-1.52	-1.45	-1.66	-1.60	-2.08
	$\Delta E(CP)$	-1.45	-0.97	-0.93	-1.10	-1.04	-1.39
	$\Delta\Delta E$	0.67	0.55	0.52	0.56	0.56	0.69
	$\Delta\Delta E$	0.63	0.47	0.45	0.54	0.48	0.64
6-311++G(3df,2p) <sup>a</sup>	$\Delta E$	-2.23	-1.59	-1.47	-1.74	-1.64	-2.19
	$\Delta E(CP)$	-1.60	-1.12	-1.02	-1.20	-1.16	-1.55
	$\Delta\Delta E$	0.63	0.47	0.45	0.54	0.48	0.64
	$\Delta\Delta E$	0.63	0.47	0.45	0.54	0.48	0.64
aug-cc-pVTZ <sup>b</sup>	$\Delta E$	-2.03	-1.44	-1.34	-1.54	-1.48	-2.00
	$\Delta E(CP)$	-1.75	-1.21	-1.12	-1.31	-1.25	-1.70
	$\Delta\Delta E$	0.28	0.23	0.22	0.23	0.23	0.30
	$\Delta\Delta E$	0.28	0.23	0.22	0.23	0.23	0.30

<sup>a</sup> Taken from ref 16. <sup>b</sup> This work.

cm<sup>-1</sup>.<sup>40</sup> The frequency of the weakly infrared-allowed F–F stretching mode of the NH<sub>3</sub>–F<sub>2</sub> complex in solid Ar has been observed experimentally at 781 cm<sup>-1</sup>,<sup>4</sup> red-shifted by -111 cm<sup>-1</sup> relative to the Raman-active F<sub>2</sub> stretching frequency of 892 cm<sup>-1</sup> in solid Ar.<sup>41</sup> The frequencies of the five intermolecular modes, two of them degenerate in pairs, could so far not be determined experimentally. The MP2 values for the intermolecular stretching frequency obtained in this work are in good agreement with earlier MP2 calculations in which the 2D energy surface spanned by the intramolecular F–F stretch and the intermolecular stretch has been subjected to harmonic and anharmonic analyses.<sup>11</sup>

**NH<sub>3</sub>–ClF.** In Tables 6 and 7, the computed  $R(N\cdots Cl)$  and  $R(Cl-F)$  distances are collected. In agreement with experiment, the computed intermolecular distance in NH<sub>3</sub>–ClF is much

shorter than in NH<sub>3</sub>–F<sub>2</sub>. The experimentally determined  $R(N\cdots Cl)$  value is 2.37(1) Å,<sup>2</sup> which was derived under the assumption of a frozen NH<sub>3</sub> monomer and a ClF subunit elongated by 0.02 Å relative to the free ClF monomer. The best computed value in this work (CCSD(T)/aug-cc-pVTZ; CP-corrected) is 2.35 Å, accompanied by an elongation of the intramolecular Cl–F distance by 0.056 Å, considerably larger than the corresponding computed elongation of F<sub>2</sub>. The HNH bond angles in the complex are widened by about 2° relative to the free NH<sub>3</sub> molecule. In contrast to the NH<sub>3</sub>–F<sub>2</sub> case just discussed, the MP2 and CCSD(T) computed intermolecular distances  $R(N\cdots Cl)$  differ by about 0.1 Å, with MP2 leading to a too short distance, while all the other electron correlation methods lead to distances too large by 0.05–0.1 Å. Again, within a given basis set, the effect of taking the CP correction



**TABLE 5: Calculated MP2 Harmonic Vibrational Frequencies, Frequency Shifts Relative to the Monomer, and Infrared Intensities of the CT Complex NH<sub>3</sub>–F<sub>2</sub><sup>a</sup>**

type of mode	symmetry	6-311++G(2d,2p)	6-311++G(3df,2p)	aug-cc-pVTZ
deg. N–H stretch	E	3670 (–3) [20]	3675 (–3) [24]	3650 (0) [22]
N–H stretch	A <sub>1</sub>	3529 (–4) [1]	3528 (–4) [1]	3502 (–1) [1]
deg. deformation	E	1688 (–4) [33]	1670 (–2) [37]	1668 (–1) [32]
deformation	A <sub>1</sub>	1068 (7) [142]	1041 (8) [149]	1046 (8) [136]
F–F stretch	A <sub>1</sub>	893 (–71) [13]	907 (–82) [13]	932 (–106) [10]
intermolecular bend	E	185 [63]	183 [48]	170 [45]
intermolecular stretch	A <sub>1</sub>	90 [3]	101 [3]	96 [2]
intermolecular bend	E	75 [50]	79 [52]	68 [52]

<sup>a</sup> Frequencies and shifts relative to the monomers (in parentheses) in cm<sup>–1</sup>; infrared intensities in square brackets in km mol<sup>–1</sup>.**TABLE 6: Calculated R(N···Cl) Distances of the CT Complex NH<sub>3</sub>–ClF As Obtained with Different Electron Correlation Methods, with Different Basis Sets, and without, R(N···Cl), and with, R<sub>CP</sub>(N···Cl), CP Correction (Å)**

basis set		MP2	MP3	MP4(DQ)	MP4(SDQ)	CCSD	CCSD(T)
6-31++G(d,p)	R(N···Cl)	2.34	2.49	2.50	2.46	2.48	2.43
	R <sub>CP</sub> (N···Cl)	2.43	2.58	2.59	2.55	2.57	2.52
	ΔR(CP)	0.09	0.09	0.09	0.09	0.09	0.09
6-311++G(2d,2p)	R(N···Cl)	2.24	2.42	2.42	2.37	2.39	2.33
	R <sub>CP</sub> (N···Cl)	2.31	2.49	2.50	2.45	2.46	2.40
	ΔR(CP)	0.07	0.07	0.08	0.08	0.07	0.07
6-311++G(3df,2p)	R(N···Cl)	2.23	2.41	2.43	2.38	2.40	2.33
	R <sub>CP</sub> (N···Cl)	2.28	2.47	2.49	2.45	2.46	2.38
	ΔR(CP)	0.05	0.06	0.06	0.07	0.06	0.05
aug-cc-pVTZ	R(N···Cl)	2.24	2.41	2.42	2.37	2.39	2.32
	R <sub>CP</sub> (N···Cl)	2.26	2.43	2.45	2.40	2.42	2.35
	ΔR(CP)	0.02	0.02	0.03	0.03	0.03	0.03

**TABLE 7: Calculated R(Cl–F) Distances of the CT Complex NH<sub>3</sub>–ClF As Obtained with Different Electron Correlation Methods, with Different Basis Sets, and without, R(ClF), and with, R<sub>CP</sub>(ClF), CP Correction (Å)**

basis set		MP2	MP3	MP4(DQ)	MP4(SDQ)	CCSD	CCSD(T)
6-31++G(d,p)	R(ClF)	1.730	1.693	1.694	1.710	1.702	1.722
	R <sub>CP</sub> (ClF)	1.720	1.689	1.690	1.704	1.698	1.718
	ΔR(CP)	0.010	0.004	0.004	0.006	0.004	0.004
	ΔR <sub>mon</sub> <sup>a</sup>	0.050	0.026	0.025	0.032	0.029	0.039
6-311++G(2d,2p)	R(ClF)	1.747	1.697	1.697	1.716	1.708	1.738
	R <sub>CP</sub> (ClF)	1.736	1.691	1.691	1.708	1.697	1.728
	ΔR(CP)	0.011	0.006	0.006	0.008	0.011	0.010
	ΔR <sub>mon</sub>	0.072	0.035	0.034	0.044	0.035	0.053
6-311++G(3df,2p)	R(ClF)	1.710	1.661	1.661	1.679	1.671	1.698
	R <sub>CP</sub> (ClF)	1.702	1.658	1.657	1.671	1.666	1.692
	ΔR(CP)	0.008	0.003	0.004	0.008	0.005	0.006
	ΔR <sub>mon</sub>	0.069	0.033	0.031	0.038	0.036	0.049
aug-cc-pVTZ	R(ClF)	1.714	1.667	1.668	1.682	1.676	1.705
	R <sub>CP</sub> (ClF)	1.712	1.665	1.666	1.680	1.674	1.702
	ΔR(CP)	0.002	0.002	0.002	0.002	0.002	0.003
	ΔR <sub>mon</sub>	0.077	0.036	0.036	0.043	0.040	0.056

<sup>a</sup> Lengthening of R(Cl–F) in the complex (with CP correction) relative to the ClF monomer.

into account in the course of the geometry optimization remains nearly constant for all methods. Despite the shorter intermolecular distance, this correction is, in general, smaller than in the NH<sub>3</sub>–F<sub>2</sub> case. This is most probably connected with the stronger interaction energy and the steeper potential in the NH<sub>3</sub>–ClF case. The computed interaction energies are reported in Table 8. The CCSD(T)-computed and CP-corrected interaction energies lie between the MP2 answers and the results as obtained with the other four electron correlation methods. Even with the aug-cc-pVTZ basis, the CP correction is with 0.7 kcal/mol still uncomfortably large. The difference between the MP2 and CCSD(T) computed stabilization energies is with about 1.5 kcal mol<sup>–1</sup> quite significant. The best computed value of the total interaction energy amounts to –9.4 kcal mol<sup>–1</sup>.

The calculated vibrational spectra of NH<sub>3</sub>–ClF are compiled in Table 9. The shifts of the three higher-lying NH<sub>3</sub> modes are still small, their infrared intensities are, however, considerably larger than in the NH<sub>3</sub>–F<sub>2</sub> complex. The frequency of the totally

symmetric NH<sub>3</sub> deformation mode in the NH<sub>3</sub>–ClF complex is substantially blue-shifted by 65 cm<sup>–1</sup> relative to that of the NH<sub>3</sub> molecule. Compared to the isolated ClF molecule, the intramolecular Cl–F stretching frequency in the complex is red-shifted by –174 cm<sup>–1</sup>, its infrared intensity is increased by about a factor of 6. The corresponding experimental shift in an Ar matrix amounts to –170 cm<sup>–1</sup>.<sup>5</sup> In that case, even the absolute values of the theoretical harmonic Cl–F stretching frequencies are close to the experimental values. The MP2/aug-cc-pVTZ computed harmonic ClF monomer stretching frequency is computed at 800 cm<sup>–1</sup>, the experimental harmonic and the fundamental frequencies are 786 and 773 cm<sup>–1</sup>, respectively.<sup>40</sup> All intermolecular modes of the NH<sub>3</sub>–ClF complex lie at much higher frequencies than those of the NH<sub>3</sub>–F<sub>2</sub> complex, despite the larger mass of the ClF molecule, a consequence of the much more attractive interaction energy in NH<sub>3</sub>–ClF.

**NH<sub>3</sub>–Cl<sub>2</sub>.** The calculated structural, energetic, and vibrational spectroscopic results for the NH<sub>3</sub>–Cl<sub>2</sub> complex are reported in

**TABLE 8: Calculated Stabilization Energies of the CT Complex NH<sub>3</sub>–ClF As Obtained with Different Electron Correlation Methods, with Different Basis Sets, and without,  $\Delta E$ , and with,  $\Delta E(\text{CP})$ , CP Correction (kcal mol<sup>-1</sup>)**

basis set		MP2	MP3	MP4(DQ)	MP4(SDQ)	CCSD	CCSD(T)
6-31++G(d,p)	$\Delta E$	-11.35	-8.90	-8.70	-9.43	-9.05	-10.08
	$\Delta E(\text{CP})$	-9.02	-7.05	-6.92	-7.46	-7.18	-7.88
	$\Delta\Delta E$	2.33	1.85	1.78	1.97	1.87	2.20
6-311++G(2d,2p)	$\Delta E$	-12.37	-8.78	-8.49	-9.36	-9.00	-10.47
	$\Delta E(\text{CP})$	-10.54	-7.44	-7.19	-7.90	-7.63	-8.73
	$\Delta\Delta E$	1.83	1.34	1.30	1.46	1.37	1.74
6-311++G(3df,2p)	$\Delta E$	-11.99	-8.76	-8.34	-9.11	-8.78	-10.30
	$\Delta E(\text{CP})$	-10.32	-7.46	-7.09	-7.82	-7.47	-8.72
	$\Delta\Delta E$	1.67	1.30	1.25	1.29	1.31	1.58
aug-cc-pVTZ	$\Delta E$	-11.82	-8.50	-8.06	-8.87	-8.53	-10.11
	$\Delta E(\text{CP})$	-10.96	-7.89	-7.48	-8.24	-7.93	-9.38
	$\Delta\Delta E$	0.86	0.61	0.58	0.63	0.63	0.73

**TABLE 9: Calculated MP2 Harmonic Vibrational Frequencies, Frequency Shifts Relative to the Monomer, and Infrared Intensities of the CT Complex NH<sub>3</sub>–ClF<sup>a</sup>**

type of mode	symmetry	6-311++G(2d,2p)	6-311++G(3df,2p)	aug-cc-pVTZ
deg. N–H stretch	E	3675 (2) [78]	3676 (-2) [81]	3653 (2) [76]
N–H stretch	A <sub>1</sub>	3527 (-6) [17]	3521 (-11) [16]	3497 (-6) [14]
deg. deformation	E	1673 (-19) [51]	1659 (-13) [55]	1657 (-12) [51]
deformation	A <sub>1</sub>	1130 (69) [142]	1095 (62) [123]	1103 (65) [114]
Cl–F stretch	A <sub>1</sub>	596 (-155) [227]	619 (-177) [237]	626 (-174) [232]
intermolecular bend	E	528 [46]	513 [34]	510 [34]
intermolecular stretch	A <sub>1</sub>	248 [107]	232 [104]	237 [104]
intermolecular bend	E	207 [8]	212 [10]	206 [10]

<sup>a</sup> Frequencies and shifts relative to the monomers (in parentheses) in cm<sup>-1</sup>; infrared intensities in square brackets in km mol<sup>-1</sup>.**TABLE 10: Calculated  $R(\text{N}\cdots\text{Cl})$  Distances of the CT Complex NH<sub>3</sub>–Cl<sub>2</sub> As Obtained with Different Electron Correlation Methods, with Different Basis Sets, and without,  $R(\text{N}\cdots\text{Cl})$ , and with,  $R_{\text{CP}}(\text{N}\cdots\text{Cl})$ , CP Correction (Å)**

basis set		MP2	MP3	MP4(DQ)	MP4(SDQ)	CCSD	CCSD(T)
6-31++G(d,p)	$R(\text{N}\cdots\text{Cl})$	2.63	2.74	2.77	2.73	2.75	2.68
	$R_{\text{CP}}(\text{N}\cdots\text{Cl})$	2.80	2.87	2.89	2.87	2.88	2.83
	$\Delta R(\text{CP})$	0.17	0.13	0.12	0.14	0.13	0.15
6-311++G(2d,2p)	$R(\text{N}\cdots\text{Cl})$	2.55	2.71	2.74	2.71	2.71	2.63
	$R_{\text{CP}}(\text{N}\cdots\text{Cl})$	2.66	2.83	2.85	2.83	2.84	2.75
	$\Delta R(\text{CP})$	0.11	0.12	0.11	0.12	0.13	0.12
6-311++G(3df,2p)	$R(\text{N}\cdots\text{Cl})$	2.61	2.73	2.76	2.73	2.74	2.66
	$R_{\text{CP}}(\text{N}\cdots\text{Cl})$	2.70	2.84	2.87	2.84	2.85	2.77
	$\Delta R(\text{CP})$	0.09	0.11	0.11	0.11	0.11	0.11
aug-cc-pVTZ	$R(\text{N}\cdots\text{Cl})$	2.59					2.64 <sup>a</sup>
	$R_{\text{CP}}(\text{N}\cdots\text{Cl})$	2.63					2.68 <sup>a</sup>
	$\Delta R(\text{CP})$	0.04					0.04 <sup>a</sup>

<sup>a</sup> Estimated.**TABLE 11: Calculated  $R(\text{Cl}–\text{Cl})$  Distances of the CT Complex NH<sub>3</sub>–Cl<sub>2</sub> As Obtained with Different Electron Correlation Methods, with Different Basis Sets, and without,  $R(\text{ClCl})$ , and with,  $R_{\text{CP}}(\text{ClCl})$ , CP Correction (Å)**

basis set		MP2	MP3	MP4(DQ)	MP4(SDQ)	CCSD	CCSD(T)
6-31++G(d,p)	$R(\text{ClCl})$	2.056	2.054	2.050	2.058	2.055	2.077
	$R_{\text{CP}}(\text{ClCl})$	2.047	2.048	2.046	2.050	2.049	2.068
	$\Delta R(\text{CP})$	0.009	0.006	0.004	0.008	0.006	0.009
	$\Delta R_{\text{mon}}^a$	0.029 <sup>a</sup>	0.020	0.017	0.018	0.017	0.026
6-311++G(2d,2p)	$R(\text{ClCl})$	2.070	2.060	2.056	2.061	2.061	2.079
	$R_{\text{CP}}(\text{ClCl})$	2.059	2.055	2.050	2.058	2.055	2.071
	$\Delta R(\text{CP})$	0.011	0.006	0.006	0.008	0.011	0.010
	$\Delta R_{\text{mon}}$	0.030	0.016	0.013	0.019	0.016	0.023
6-311++G(3df,2p)	$R(\text{ClCl})$	2.017	2.019	2.015	2.018	2.018	2.032
	$R_{\text{CP}}(\text{ClCl})$	2.011	2.013	2.010	2.013	2.013	2.025
	$\Delta R(\text{CP})$	0.006	0.006	0.005	0.005	0.005	0.007
	$\Delta R_{\text{mon}}$	0.027	0.016	0.016	0.015	0.016	0.020
aug-cc-pVTZ	$R(\text{ClCl})$	2.034					2.049 <sup>b</sup>
	$R_{\text{CP}}(\text{ClCl})$	2.028					2.043 <sup>b</sup>
	$\Delta R(\text{CP})$	0.006					0.006 <sup>b</sup>
	$\Delta R_{\text{mon}}$	0.035					0.030 <sup>b</sup>

<sup>a</sup> Lengthening of  $R(\text{Cl}–\text{Cl})$  in the complex (with CP correction) relative to the Cl<sub>2</sub> monomer. <sup>b</sup> Estimated.

Tables 10–13. The general trends observed for this complex are very similar to that of the NH<sub>3</sub>–F<sub>2</sub> complex. As already mentioned before, the NH<sub>3</sub>–Cl<sub>2</sub> complex could not be treated at post-MP2 levels when using the aug-cc-pVTZ basis. How-

ever, with the aid of the results on the two other complexes, the MP2/aug-cc-pVTZ data, and the calculations with the three smaller basis sets, a quite reliable estimate is possible for the CCSD(T)/aug-cc-pVTZ numbers. The estimated intermolecular

**TABLE 12: Calculated Stabilization Energies of the CT Complex NH<sub>3</sub>–Cl<sub>2</sub> As Obtained with Different Electron Correlation Methods, with Different Basis Sets, and without,  $\Delta E$ , and with,  $\Delta E(\text{CP})$ , CP Correction (kcal mol<sup>−1</sup>)**

basis set		MP2	MP3	MP4(DQ)	MP4(SDQ)	CCSD	CCSD(T)
6-31++G(d,p)	$\Delta E$	−5.58	−4.64	−4.35	−4.65	−4.53	−5.21
	$\Delta E(\text{CP})$	−3.81	−3.17	−2.99	−3.17	−3.09	−3.48
	$\Delta\Delta E$	1.77	1.47	1.36	1.48	1.44	1.73
6-311++G(2d,2p)	$\Delta E$	−6.17	−4.73	−4.39	−4.70	−4.61	−5.41
	$\Delta E(\text{CP})$	−4.71	−3.62	−3.37	−3.59	−3.53	−4.05
	$\Delta\Delta E$	1.46	1.11	1.02	1.11	1.08	1.36
6-311++G(3df,2p)	$\Delta E$	−6.03	−4.90	−4.51	−4.79	−4.71	−5.53
	$\Delta E(\text{CP})$	−4.47	−3.57	−3.28	−3.49	−3.44	−4.02
	$\Delta\Delta E$	1.56	1.33	1.23	1.30	1.25	1.41
aug-cc-pVTZ	$\Delta E$	−5.46					−4.96 <sup>a</sup>
	$\Delta E(\text{CP})$	−4.92					−4.42 <sup>a</sup>
	$\Delta\Delta E$	0.54					0.54 <sup>a</sup>

<sup>a</sup> Estimated.**TABLE 13: Calculated MP2 Harmonic Vibrational Frequencies, Frequency Shifts Relative to the Monomer, and Infrared Intensities of the CT Complex NH<sub>3</sub>–Cl<sub>2</sub><sup>a</sup>**

type of mode	symmetry	6-311++G(2d,2p)	6-311++G(3df,2p)	aug-cc-pVTZ
deg. N–H stretch	E	3673 (0) [42]	3674 (−4) [40]	3649 (−1) [38]
N–H stretch	A <sub>1</sub>	3527 (−6) [5]	3523 (−9) [7]	3498 (−5) [2]
deg. deformation	E	1681 (−11) [44]	1665 (−7) [44]	1663 (−6) [20]
deformation	A <sub>1</sub>	1078 (17) [107]	1050 (17) [125]	1060 (22) [108]
Cl–Cl stretch	A <sub>1</sub>	484 (−56) [61]	511 (−67) [42]	505 (−68) [45]
intermolecular bend	E	327 [54]	283 [46]	287 [46]
intermolecular stretch	A <sub>1</sub>	152 [51]	146 [30]	138 [34]
intermolecular bend	E	116 [17]	103 [17]	100 [9]

<sup>a</sup> Frequencies and shifts relative to the monomers (in parentheses) in cm<sup>−1</sup>; infrared intensities in square brackets in km mol<sup>−1</sup>.

$R(\text{N}\cdots\text{Cl})$  distance amounts to 2.68 Å, somewhat shorter than the experimental value of  $2.73 \pm 0.03$  Å.<sup>3</sup> Compared to the free Cl<sub>2</sub> molecule an increase of the intramolecular Cl–Cl is distance in the complex by about 0.03 Å is calculated. The HNH bond angles are widened by about 0.7°. The CCSD(T)/aug-cc-pVTZ interaction energy is estimated as −4.4 kcal mol<sup>−1</sup>.

Experimental vibrational spectra are not available for the NH<sub>3</sub>–Cl<sub>2</sub> complex. The calculated intramolecular NH<sub>3</sub> vibrations of the complex show shifts qualitatively similar to those in the NH<sub>3</sub>–F<sub>2</sub> case. The infrared intensities of these four modes and that of the Cl–Cl stretching mode are halfway between that of the NH<sub>3</sub>–F<sub>2</sub> and NH<sub>3</sub>–ClF complexes. The computed red shift of the intramolecular Cl–Cl stretching frequency amounts to −68 cm<sup>−1</sup>. The three intermolecular modes are all higher than in the complex with F<sub>2</sub>. Thus, the stronger binding overcompensates the larger mass of Cl<sub>2</sub>.

**Trends in the Series NH<sub>3</sub>–F<sub>2</sub>, NH<sub>3</sub>–ClF, and NH<sub>3</sub>–Cl<sub>2</sub>.** Rather than to try to establish the amount of charge transfer between NH<sub>3</sub> and the halogens directly, which is a notoriously difficult problem, a pragmatic point of view is taken to illustrate the strength and the character of the interaction in this series. The trends in several expectation values thought to be connected with the strength of the intermolecular interaction are monitored and discussed in the following. The structural, energetic, and vibrational properties as obtained with the aug-cc-pVTZ basis at CCSD(T) and MP2 levels for the three complexes are recollected. In addition to these data, MP2/aug-cc-pVTZ-calculated zero point energy (ZPE) corrections, ZPE-corrected stabilization energies, dipole moments, dipole moment enhancements relative to the sum of monomer dipole moments, the harmonic force constants of the 2 × 2 submatrix spanned by  $R(\text{X}–\text{Y})$  and  $R(\text{N}\cdots\text{X})$ , the diagonal harmonic force constants for the bending of the linear N $\cdots$ X–Y subunit and for the bending of the C<sub>3</sub> axis of the NH<sub>3</sub> molecule relative to the N $\cdots$ X connection, and, finally, electric field gradients on N, F, and Cl atoms together with the nuclear quadrupole coupling constants  $\chi(^{14}\text{N})$  and  $\chi(^{35}\text{Cl})$  are shown in Table 14.

**TABLE 14: Trends in Selected Ground-State Expectation Values in the Series NH<sub>3</sub>–XY As Obtained at the CCSD(T) and MP2/aug-cc-pVTZ Level**

property	NH <sub>3</sub> –F <sub>2</sub>	NH <sub>3</sub> –ClF	NH <sub>3</sub> –Cl <sub>2</sub>
$R(\text{N}\cdots\text{X})$ (Å)	2.67	2.35	2.68
$\Delta R(\text{X}–\text{Y})$ (Å) <sup>a</sup>	0.012	0.056	0.030
$\Delta E$ (kcal mol <sup>−1</sup> )	−1.70	−9.38	−4.42
$\Delta E(\text{ZPE})$ (kcal mol <sup>−1</sup> ) <sup>b</sup>	−0.97	−7.18	−3.22
$\angle\text{HNH}$ (deg) <sup>c</sup>	106.9	108.9	107.5
$\Delta\angle\text{HNH}$ (deg) <sup>c</sup>	0.1	2.1	0.7
$\mu$ (D) <sup>c</sup>	1.99	5.67	3.40
$\Delta\mu$ (D) <sup>c,d</sup>	0.47	3.23	1.88
$\Delta\nu(\text{X}–\text{Y})$ (cm <sup>−1</sup> ) <sup>c</sup>	−106	−174	−68
$\nu(\text{N}\cdots\text{X})$ (cm <sup>−1</sup> ) <sup>c</sup>	96	237	138
$f(\text{X}–\text{Y})$ (mdyn Å <sup>−1</sup> ) <sup>c</sup>	5.06	3.13	2.85
$f(\text{X}–\text{Y}/\text{N}\cdots\text{X})$ (mdyn Å <sup>−1</sup> ) <sup>c</sup>	0.21	0.55	0.26
$f(\text{N}\cdots\text{X})$ (mdyn Å <sup>−1</sup> ) <sup>c</sup>	0.07	0.50	0.17
$\Delta f(\text{X}–\text{Y})$ (mdyn Å <sup>−1</sup> ) <sup>c</sup>	−0.62	−1.51	−0.83
$f(\text{N}\cdots\text{X}–\text{Y})$ (mdyn Å) <sup>c</sup>	0.087	0.63	0.27
$f(\text{H}_3\text{N}\cdots\text{X})$ (mdyn Å) <sup>e</sup>	0.0096	0.13	0.041
efg N (au) <sup>c</sup>	0.783 (−3.72) <sup>f</sup>	0.569 (−2.70) <sup>f</sup>	0.719 (−3.41) <sup>f</sup>
efg X (au) <sup>c</sup>	−6.17	−7.09 (−136) <sup>g</sup>	−5.74 (−110) <sup>g</sup>
efg Y (au) <sup>c</sup>	−5.86	−3.21	−4.90 (−94) <sup>g</sup>

<sup>a</sup> Lengthening of  $R(\text{X}–\text{Y})$  relative to the monomer. <sup>b</sup> ZPE- and CP-corrected CCSD(T) interaction energy; ZPE corrections from MP2/aug-cc-pVTZ frequencies. <sup>c</sup> MP2/aug-cc-pVTZ. <sup>d</sup> Difference to the sum of monomer dipole moments. <sup>e</sup> Diagonal force constant for tilting the C<sub>3</sub> axis of NH<sub>3</sub> relative to N $\cdots$ X connection. <sup>f</sup> Values in parentheses are nuclear quadrupole coupling constants  $\chi(^{14}\text{N})$  in MHz. <sup>g</sup> Values in parentheses are nuclear quadrupole coupling constants  $\chi(^{35}\text{Cl})$  in MHz.

The most important computed quantity is the intermolecular distance  $R(\text{N}\cdots\text{X})$  because it can be reliably determined from the experimental side. The CP-corrected and CCSD(T)/aug-cc-pVTZ-calculated values of 2.67 Å for NH<sub>3</sub>–F<sub>2</sub>, 2.35 Å for NH<sub>3</sub>–ClF, and 2.68 Å for NH<sub>3</sub>–Cl<sub>2</sub> are satisfactorily close and consistently below the corresponding experimentally deduced values of 2.71,<sup>1</sup> 2.37,<sup>2</sup> and 2.73<sup>3</sup> Å, respectively. Compared to previous calculations on these complexes, the agreement with



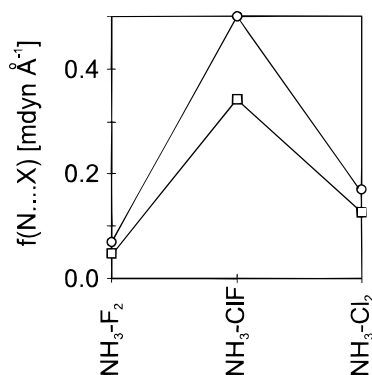


**Figure 5.** Comparison of MP2/aug-cc-pVTZ-calculated harmonic force constants  $f(\text{N}\cdots\text{X})$ , open circles, with experimentally deduced values, open squares. Experimental values taken from refs 1–3.

the rotational spectroscopic data is considerably improved. In this series, the widening of the HNH bond angles in the complexes display the same trends as the other structural parameters. The computed modifications of the HNH bond angles range from 0.1° in NH<sub>3</sub>-F<sub>2</sub> to about 2.0° in NH<sub>3</sub>-ClF, with an intermediate value of 0.7° in NH<sub>3</sub>-Cl<sub>2</sub>. The assumption of frozen monomers often used in the interpretation of the rotational spectroscopic data appears to be justified for the NH<sub>3</sub> subunit in all three complexes. The computed elongation of the ClF bond of 0.056 Å is a bit larger than the 0.02 Å assumed in ref 2 on the basis of an earlier ab initio calculation. It should be stressed that effects due to vibrational averaging over intermolecular coordinates are not treated in this work.

An important expectation value to characterize charge transfer is the dipole moment of the complex. Experimental dipole moments are not yet available. The computed dipole moment is largest in the case of NH<sub>3</sub>-ClF and smallest for NH<sub>3</sub>-F<sub>2</sub>. The same order occurs for the dipole moment increase relative to the sum of monomer dipole moments. Suitable indicators for the strength of interaction are the shifts of the intramolecular modes, in particular of the X–Y stretching frequency, and the frequency of the intermolecular stretching mode. While the latter behaves in this series as the other properties discussed so far, there appears to be a small deviation from the general trend when inspecting the trends for the shift of the X–Y stretching frequency. Again, this red shift is largest for NH<sub>3</sub>-ClF, but the relative order is reversed for the other two complexes. This is, however, merely a consequence of the much lower-lying vibrational frequency of Cl<sub>2</sub> as compared to that of F<sub>2</sub>. A detailed analysis of the 2 × 2 harmonic fields reveals that the decrease of the intramolecular stretching force constant  $\Delta f(\text{X}-\text{Y})$  obeys the expected order. From the experimental analysis of centrifugal distortions,<sup>1–3</sup> effective intermolecular force constants have been determined for these three complexes. Values of 0.047, 0.343, and 0.127 mdyn Å<sup>-1</sup> have been reported. While these force constants cannot be compared directly to the harmonic  $f(\text{N}\cdots\text{X})$  values reported in Table 14, for a number of reasons, the two sets of values correlate quite nicely as shown in Figure 5.

Apart from the stretching degrees of freedom, the intermolecular bending frequencies and the bending force constants  $f(\text{N}\cdots\text{X}-\text{Y})$  and  $f(\text{H}_3\text{N}\cdots\text{X})$ , the latter describing the tilt of the C<sub>3</sub> axis of NH<sub>3</sub> relative to the N $\cdots$ X bond, provide also useful insight into the intermolecular bonding and the flexibility of these complexes. There are two degenerate pairs of bending frequencies, one lower and one higher than the intermolecular stretching frequency. Those of the lower bending frequency are computed at 68, 206, and 100 cm<sup>-1</sup> for the complexes with F<sub>2</sub>, ClF, and Cl<sub>2</sub> at the MP2/aug-cc-pVTZ level. The frequencies

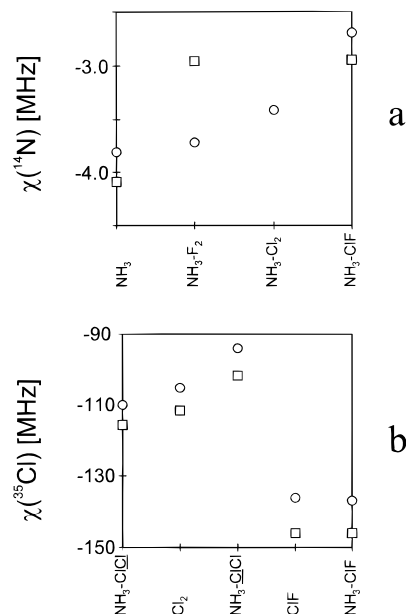


**Figure 6.** Comparison of calculated and experimental quadrupole coupling constants  $\chi(^{14}\text{N})$  (a) and  $\chi(^{35}\text{Cl})$  (b): (squares) Experimental values taken from refs 1–3 and 42–44; (circles) MP2/aug-cc-pVTZ computed.

of the higher-lying bending mode are computed at 170, 510, and 287 cm<sup>-1</sup>, respectively. The force constants  $f(\text{N}\cdots\text{X}-\text{Y})$  and  $f(\text{H}_3\text{N}\cdots\text{X})$  in this series show the varying angular flexibility of these complexes in an even more clear fashion.

Other interesting quantities which are often used to characterize the intermolecular interaction are the nuclear quadrupole coupling constants  $\chi$ . These may be evaluated from computed electric field gradients on the nuclei. Experimental quadrupole coupling constants are available for <sup>14</sup>N in the case of NH<sub>3</sub>-F<sub>2</sub><sup>1</sup> and NH<sub>3</sub>-ClF,<sup>2</sup> and also for free NH<sub>3</sub>.<sup>42</sup> Moreover, <sup>35</sup>Cl nuclear quadrupole coupling constants have also been determined for NH<sub>3</sub>-ClF,<sup>2</sup> NH<sub>3</sub>-Cl<sub>2</sub>,<sup>3</sup> ClF,<sup>43</sup> and Cl<sub>2</sub>.<sup>44</sup> Strictly taken, the direct comparison between experimental and computed values for  $\chi(^{14}\text{N})$  and  $\chi(^{35}\text{Cl})$  is not possible without additional assumptions because the experimental quantities correspond to vibrational averages over the large-amplitude intermolecular bending coordinates. From their experimental work, Legon and co-workers<sup>1–3</sup> derived values for NH<sub>3</sub>-F<sub>2</sub>, NH<sub>3</sub>-ClF, and NH<sub>3</sub>-Cl<sub>2</sub> of 25, 15, and 15° for the average bending of the C<sub>3</sub> axis of NH<sub>3</sub> relative to the line connecting the center of masses of NH<sub>3</sub> and the halogen and values of 20, 10, and 7.5° for the average bending of the halogen axis relative to the line connecting the center of masses of NH<sub>3</sub> and the halogen. In Figure 6, the computed  $\chi(^{14}\text{N})$  and  $\chi(^{35}\text{Cl})$  are, nevertheless, confronted with the experimental values. In the case of  $\chi(^{35}\text{Cl})$  (see Figure 6b) this averaging is probably less problematic because of the larger mass of the halogen and the smaller angular distortions. The description of the changes brought about by the intermolecular interaction and the difference between ClF and Cl<sub>2</sub> molecules appear to be well described, although the computed values are all too high by about 5–8 MHz. In the case of  $\chi(^{14}\text{N})$  (see Figure 6a), the agreement between computed (nonaveraged) and experimental values appears acceptable in the cases of NH<sub>3</sub> and NH<sub>3</sub>-ClF, but there is a large discrepancy for NH<sub>3</sub>-F<sub>2</sub>, the origin of which is most probably the soft bending potential in that weakly bound complex, which gives rise to the large angular distortions, as discussed in the experimental work.<sup>1</sup>

## Summary and Conclusions

A large-scale systematic study of the three heterodimers NH<sub>3</sub>-F<sub>2</sub>, NH<sub>3</sub>-ClF, and NH<sub>3</sub>-Cl<sub>2</sub> has been presented. An excellent agreement between experimentally determined structures and CP-corrected CCSD(T)/aug-cc-pVTZ-optimized geometries is achieved. Because the CP correction is still nonnegligible at this level of approximation, it has to be taken into account in the process of geometry optimization. The sensitivity of the computed geometry parameters to the basis set and electron correlation method chosen, as observed previously for the case of NH<sub>3</sub>-F<sub>2</sub>, persists also for the other two complexes. From all other correlation methods probed, the MP2 results are closest to the CCSD(T) answers. The very close agreement between these two approaches appears, however, fortuitous in the case of NH<sub>3</sub>-F<sub>2</sub>. In the other two cases the MP2 computed distances are too short. All computed quantities point to an increase of the intermolecular interaction in the order NH<sub>3</sub>-F<sub>2</sub>, NH<sub>3</sub>-Cl<sub>2</sub>, and NH<sub>3</sub>-ClF.

**Acknowledgment.** The calculations were performed on the Cluster of Digital Alpha Servers (2100 4/275 and 5/375) of the computer center of the University of Vienna and on local RISC 6000/550 and Silicon Graphics workstations at the Institute of Theoretical Chemistry and Molecular Structural Biology of the University of Vienna. The author is grateful for an ample supply of computer time on these installations.

## References and Notes

- (1) Bloemink, H. I.; Hinds, K.; Holloway, J. H.; Legon, A. C. *Chem. Phys. Lett.* **1995**, 245, 598.
- (2) Bloemink, H. I.; Evans, C. M.; Holloway, J. H.; Legon, A. C. *Chem. Phys. Lett.* **1996**, 248, 260.
- (3) Legon, A. C.; Lister, D. G.; Thorn, J. C. *J. Chem. Soc., Faraday Trans.* **1994**, 90, 3205.
- (4) Andrews, L.; Lascola, R. *J. Am. Chem. Soc.* **1987**, 109, 6243.
- (5) Machara, N. P.; Ault, B. S. *J. Phys. Chem.* **1988**, 92, 2439.
- (6) Lucchese, R. R.; Schaefer, H. F., III. *J. Am. Chem. Soc.* **1975**, 97, 7205.
- (7) Umeyama, H.; Morokuma, K.; Yamabe, S. *J. Am. Chem. Soc.* **1977**, 99, 330.
- (8) Reed, A. E.; Weinhold, F.; Curtiss, L. A.; Pochatko, D. J. *Chem. Phys.* **1986**, 84, 5687.
- (9) Røeggen, I.; Dahl, T. *J. Am. Chem. Soc.* **1992**, 114, 511.
- (10) Tachikawa, H.; Komatsu, E. *Inorg. Chem.* **1995**, 34, 6546.
- (11) Latajka, Z.; Scheiner, S.; Bouteiller, Y.; Ratajczak, H. *J. Mol. Struct.* **1996**, 376, 343.
- (12) Ruiz, E.; Salahub, D. R.; Vela, A. *J. Phys. Chem.* **1996**, 100, 12265.
- (13) Zhang, Y.; Zhao, C.-Y.; You, X.-Z. *J. Phys. Chem. A* **1997**, 101, 2879.
- (14) Alkorta, I.; Rozas, J.; Elguero, J. *J. Phys. Chem. A* **1998**, 102, 9278.
- (15) Karpfen, A. *Chem. Phys. Lett.* **1999**, 299, 493.
- (16) Karpfen, A. *Chem. Phys. Lett.* **2000**, 316, 483.
- (17) Matsuzawa, H.; Iwata, S. *Chem. Phys.* **1992**, 163, 297.
- (18) Kobayashi, T.; Matsuzawa, H.; Iwata, S. *Bull. Chem. Soc. Jpn.* **1994**, 67, 3172.
- (19) Latajka, Z.; Berski, S. *J. Mol. Struct. (THEOCHEM)*. **1996**, 371, 11.
- (20) Møller, C.; Plesset, M. S. *Phys. Rev.* **1934**, 46, 618.
- (21) Boys, S. F.; Bernardi, F. *Mol. Phys.* **1970**, 19, 553.
- (22) Frisch, M. J.; Trucks, G. W.; Schlegel, H. B.; Scuseria, G. E.; Robb, M. A.; Cheeseman, J. R.; Zakrzewski, J. A.; Montgomery, J. A., Jr.; Stratmann, R. E.; Burant, J. C.; Dapprich, S.; Millam, J. M.; Daniels, A. D.; Kudin, K. N.; Strain, M. C.; Farkas, O.; Tomasi, J.; Barone, V.; Cossi, M.; Cammi, R.; Mennucci, B.; Pomelli, C.; Adamo, C.; Clifford, S.; Ochterski, J.; Petersson, G. A.; Ayala, P. Y.; Cui, Q.; Morokuma, K.; Malick, D. K.; Rabuck, A. D.; Raghavachari, K.; Foresman, J. B.; Cioslowski, J.; Ortiz, J. V.; Stefanov, B. B.; Liu, G.; Liashenko, A.; Piskorz, P.; Komaromi, I.; Gomperts, R.; Martin, R. L.; Fox, D. J.; Keith, T.; Al-Laham, M. A.; Peng, C. Y.; Nanayakkara, A.; Gonzalez, C.; Challacombe, M.; Gill, P. M. W.; Johnson, B.; Chen, W.; Wong, M. W.; Andres, J. L.; Gonzalez, C.; Head-Gordon, M.; Replogle, E. S.; Pople, J. A. *Gaussian 98*, Revision A.6; Gaussian, Inc.: Pittsburgh, PA, 1998.
- (23) Krishnan, R.; Pople, J. A. *Int. J. Quantum Chem.* **1978**, 14, 91.
- (24) Cizek, J. *Adv. Chem. Phys.* **1969**, 14, 35.
- (25) Purvis, G. D.; Bartlett, R. J. *J. Chem. Phys.* **1982**, 76, 1910.
- (26) Scuseria, G. E.; Janssen, C. L.; Schaefer, H. F., III. *J. Chem. Phys.* **1988**, 89, 7382.
- (27) Scuseria, G. E.; Schaefer, H. F., III. *J. Chem. Phys.* **1989**, 90, 3700.
- (28) Pople, J. A.; Head-Gordon, M.; Raghavachari, K. *J. Chem. Phys.* **1987**, 87, 5968.
- (29) Ditchfield, R.; Hehre, W. J.; Pople, J. A. *J. Chem. Phys.* **1971**, 54, 724.
- (30) Hehre, W. J.; Ditchfield, R.; Pople, J. A. *J. Chem. Phys.* **1972**, 56, 2257.
- (31) McLean, A. D.; Chandler, G. S. *J. Chem. Phys.* **1980**, 72, 5639.
- (32) Frisch, M. J.; Pople, J. A.; Binkley, J. S. *J. Chem. Phys.* **1984**, 80, 3265.
- (33) Krishnan, R.; Binkley, J. S.; Seeger, R.; Pople, J. A. *J. Chem. Phys.* **1980**, 72, 5639.
- (34) Clark, T.; Chandrasekhar, J.; Spitznagel, G. W.; Schleyer, P. v. R. *J. Comput. Chem.* **1983**, 4, 294.
- (35) Woon, D. E.; Dunning, Th. R., Jr. *J. Chem. Phys.* **1993**, 98, 1358.
- (36) Kendall, R. E.; Dunning, Th. R., Jr.; Harrison, R. J. *J. Chem. Phys.* **1992**, 96, 6796.
- (37) Davidson, E. R. *Chem. Phys. Lett.* **1996**, 220, 514.
- (38) Simon, S.; Duran, M.; Dannenberg, J. J. *J. Phys. Chem. A* **1999**, 103, 1640.
- (39) Hobza, P.; Bludský, O.; Suhai, S. *Phys. Chem. Chem. Phys.* **1999**, 1, 3073.
- (40) Huber, K. P.; Herzberg, G. *Molecular Spectra and Molecular Structure*, Vol. 4, *Constants of Diatomic Molecules*; Van Nostrand Reinhold: New York, 1979.
- (41) Howard, W. F., Jr.; Andrews, L. *J. Am. Chem. Soc.* **1973**, 95, 3045.
- (42) Marshall, M. D.; Muentner, J. S. *J. Mol. Spectrosc.* **1981**, 85, 322.
- (43) Fabricant, B.; Muentner, J. S. *J. Chem. Phys.* **1977**, 66, 5274.
- (44) Fowler, P. W.; Legon, A. C.; Peebles, S. A. Unpublished, as quoted in ref 3.